2mif

NASA TECHNICAL TRANSLATION NASA TT F-15,416

RESULTS OF THE COMBINED APPLICATION OF BOUNDARY LAYER AND PROFILE THEORY

Richard Eppler

Translation of "Ergebnisse gemeinsamer Anwendung von Grenzschicht- und Profiltheorie," Zeitschrift für Flugwissenschaften, Vol. 8, No. 9, Sept. 1960, pp. 247-260

(NASA-TT-F-15416) RESULTS OF THE COMBINED APPLICATION OF BOUNDARY LAYER AND PROFILE THEORY (Kanner (Leo) Associates) ~~38~~ 40 p HC $5.00 CSCL 20D N74-18917 G3/12 Unclas 32008

NATIONAL AERONAUTICS AND SPACE ADMINISTRATION
WASHINGTON, D.C. 20546 MARCH 1974

STANDARD TITLE PAGE

1. Report No. NASA TT F-15,416	2. Government Accession No.	3. Recipient's Catalog No.
4. Title and Subtitle RESULTS OF THE COMBINED APPLICATION OF BOUNDARY LAYER AND PROFILE THEORY		5. Report Date March 1974 6. Performing Organization Code
7. Author(s) Richard Eppler Bölkow-Entwicklungen KG		8. Performing Organization Report No. 10. Work Unit No.
9. Performing Organization Name and Address Leo Kanner Associates, P.O. Box 5187, Redwood City, California 94063		11. Contract or Grant No. NASw-2481 13. Type of Report and Period Covered Translation
12. Sponsoring Agency Name and Address NATIONAL AERONAUTICS AND SPACE ADMINISTRATION, WASHINGTON, D.C. 20546		14. Sponsoring Agency Code

15. Supplementary Notes

Translation of "Ergebnisse gemeinsamer Anwendung von Grenzschicht- und Profiltheorie," Zeitschrift für Flugwissenschaften, Vol. 8, No. 9, Sept. 1960, pp. 247-260.

16. Abstract Applied results of combined boundary layer and profile theory show that it is possible to determine in a simple way profiles with fixed characteristics of pressure distribution by means of which extensive boundary layer calculations can be carried out; series of profiles can be studied systematically and determination of profiles, analogous to procedure in wind tunnels, is possible; theoretical possibilities are explained with examples.

17. Key Words (Selected by Author(s))	18. Distribution Statement
	Unclassified - Unlimited

19. Security Classif. (of this report)	20. Security Classif. (of this page)	21. No. of Pages	22. Price
Unclassified	Unclassified	40	$5.00

NASA-HQ

RESULTS OF THE COMBINED APPLICATION OF BOUNDARY LAYER AND PROFILE THEORY

Richard Eppler
Bölkow-Entwicklungen KG

Summary /247*

By means of recently developed methods of calculation for boundary layer and profile theory, which have been published elsewhere, it is possible to determine in a simple way profiles with fixed characteristics of pressure distribution and to carry out with them extensive boundary layer calculations. As the results are more reliable compared to those of former ones, and as they are more quickly available because of digital computers, series of profiles can be studied systematically and a determination of profiles, which is analogous to the procedure in the wind tunnel, is possible; these profiles result in an optimum solution of certain studies within the theory. By giving examples of the pressure rise curve after boundary layer transition, of the distribution of laminar portions on the suction and pressure sides of the airfoil, and of the problem of high maximum lift, the author explains the theoretical possibilities.

1. Introduction

The combined application of boundary layer and profile theory took place already at an early date, chiefly starting, however, from fixed profiles for which pressure distribution and boundary layer were calculated. The calculations were expensive and nearly always so uncertain that they had little practical value.

With advancing development of boundary layer theory, the knowledge grew concerning the requirements for velocity distribution on profiles for a favorable development of the boundary layer. This resulted in a reversal of problems in profile theory,

*Numbers in the margin indicate pagination in the foreign text.

namely, to find profiles with specified characteristics of velocity distribution. The studies resulted in the well-known NACA laminar profiles that were destined to have great success. It is true that the profiles which had been calculated only to a limited extent did not by any means do justice to all problems; in addition, the turbulent boundary layer and the profile also had not been exhaustively dealt with.

In the meantime, more knowledge has been acquired regarding the phenomena in the boundary layer, especially the turbulent boundary layer, and today we are in possession of simpler methods of calculation in the profile and boundary layer theory.

On top of this is the considerable reduction of expenses and above all of calculating time by means of electronic computers, so that it has become possible to calculate whole series of profiles and from them to derive optimal solutions for the most varied problems at only a fraction of the expense required for wind-tunnel measurements or the construction of a wing. We will report in the following on the purely theoretical methods of this process. In the foreground of discussion will be the fact that the theory actually offers these basic possibilities and the aspect of how it works. So far, it is not possible to predict to what extent we will be successful with experimental corroboration. In any case, it will become clear that it will pay to devote some experimental attention to the entire method, as by this means it is possible under certain circumstances to get away altogether from the customary method of selecting a profile from more or less voluminous catalogs of data and to be able to calculate for any application the one suitable profile. First steps in this direction met with definite success, even though they possibly seemed somewhat rash.

2. Profile Theory, Method of Calculation

/248

Airfoils, the velocity distribution of which must have specified characteristics, require special methods of calculation. Due to the fact that in most cases certain characteristics of velocity distribution are required at quite different angles of incidence, as will be shown later in detail by means of examples, the method of calculation should permit, as far as possible, the introduction of conditions, or at least allow an easy way of keeping track of velocity distribution at the most varied angles of incidence.

The first and best-known procedure for this purpose was offered by T. Theodorsen and served for calculating the well-known NACA laminar airfoils [1]. It required, however, a very large input of calculating effort and was only used for symmetrical profiles. Cambered profiles were obtained by means of the theory of approximation of the section with turbulence distribution. Certain errors had to be put up with which, on the one hand, resulted from the theory of singularity itself, and on the other hand, from its application to finite thick profiles. In addition, the calculation of symmetrical profiles at the leading edge was connected with difficulties. It was not possible to attain complete accuracy at this location.

At a later date, profiles were calculated by J. Lighthill [2] that were obtained, both cambered and symmetrical, by means of conformal representation and in cases where it was possible to specify exactly and meet the characteristics of velocity distribution. However, this method was suitable only for especially simple analytical velocity specifications.

E. Truckenbrodt [3] presented a simple method of approximation based on singularity distribution for the solution of the same problem which, however, was limited with respect to possibilities of specification (for only one value of lift) and

accuracy and which also presented difficulties working with different angles of incidence. Consequently, another method was developed [4] which also uses conformal representation and combines the accuracy of Lighthill with general possibilities of using desired numerical values and requires less numerical effort.

The possibilities of specified values offered by the new method are made evident by the example in Fig. 1. An airfoil is shown with its distribution of velocity for four different angles of incidence. This represents the typical picture with which we are familiar from experiments and theory. With increasing angle of incidence, velocity increases on the upper surface and decreases on the lower surface. The changes in each case are greatest in the vicinity of the leading edge and practically disappear at the trailing edge. The essential feature is this: the representation exhibits some peculiarities at different angles of incidence that can be traced back to the specified conditions. Those portions of the four velocity distributions which are decisive for fixing the profile have been drawn with a heavy line in the figure. On the upper surface at an angle of incidence of $\alpha = 4.9°$, velocity is constant over a wide range. In the direction of the trailing edge, a certain decrease in

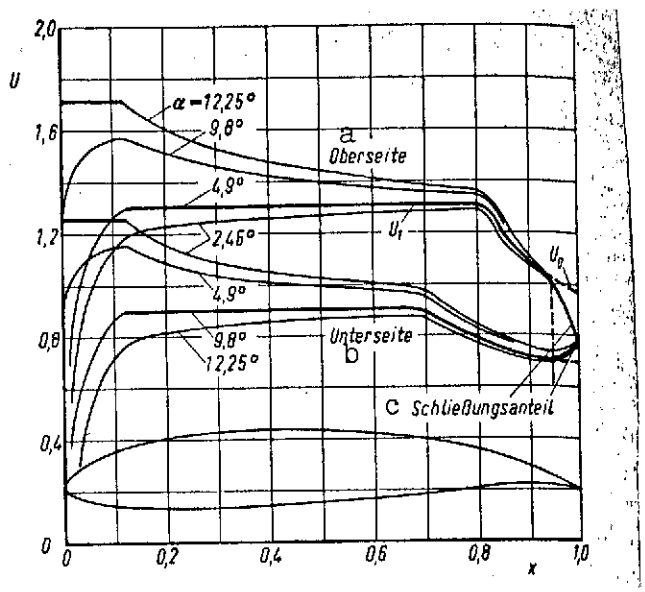

Fig. 1. Example for the profile calculating method.

Key: a. Upper surface
b. Lower surface
c. Closing component

velocity was specified, the form of which was given in relation to constant velocity. Especially the total magnitude of U_1/U_0 of the velocity decrease and the gradient U'/U can be specified at the beginning. At a high angle of incidence of 12.25°, velocity in the vicinity of the leading edge is constant on the upper surface. On the lower surface, velocity is constant in the vicinity of the leading edge at the very small angle of incidence of 2.45°, while it is constant over a larger section at 9.8°. For the aft portion of the lower surface, the form of velocity decrease is specified just as it is on the upper surface. In the immediate vicinity of the trailing edge, still other changes in velocity can be observed. In the first place, they effect continuity of velocity at the trailing edge, a condition that is a must for the exact method of calculation, as otherwise a singularity would occur. In the second place, a closure of the profile is produced by these short sections. If the profile is very thick shortly before it reaches the trailing edge, then a large rise in pressure is required at the "closing component." Conversely, it is possible to evaluate the fineness of the trailing edge by means of the closing components that are calculated prior to the actual profile, and if necessary, to affect its design by means of changes in the layout and the required thickness of the closure.

The specified angles of incidence are always in reference to the direction of zero lift. Therefore, the lift coefficients can be calculated from them by means of

$$c_A = 2\pi\eta\alpha \qquad (1)$$

in which case $\eta \geq 1$ is a quantity which depends on the thickness of the profile and can be approximated at a value equal to 1. It is part of the calculating process but plays no decisive role due to the fact that in the experiment, on account of the boundary layer cushion, about all that is just above the value of 1 is lost again.

The method of calculation introduces the heavy-lined conditions for velocity distribution in an exact manner into the methodology of conformal representation. A singularity that forms at the stagnation point was split off; also a second one that occurs in the vicinity of the leading edge due to a sharp angle or a big jump in the derivation of the speed variation. Conformal representations that were used for a backward calculation of the distribution of velocities from the airfoil yielded excellent agreement with specified values. Neither is there any /248 disturbing difference in a comparison with experimental pressure distributions.

The calculating effort is comparable to that of Truckenbrodt for the same number of calculated points. The main advantage of the method lies in the exact calculation of the leading edge. A comparison with profiles calculated in accordance with other methods demonstrates the effect of the exact calculation. Figure 2 represents an example of a calculation which solves the known problem of common laminar airfoils.

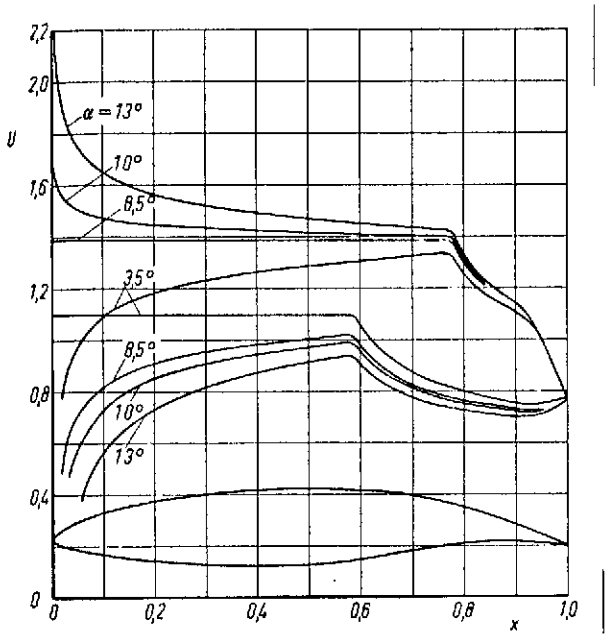

Fig. 2. Airfoil STF 863-615 in accordance with NACA 66_3-618.

On the upper surface, velocity is as follows: at $\alpha = 8.5°$ or in accordance with (1) with $\eta = 1.08$ at $c_A = 1.02$ it is constant up to $x = 0.8$; on the lower surface at $\alpha = 3.5°$ or $c_A = 0.42$, it is constant up to $x = 0.6$. In the range between these two angles of incidence, velocity increases on the upper and lower surface over the corresponding sections. The boundary layer can be maintained in a laminar condition

over these "laminar lengths," and in the polar diagram there can be expected the well-known "laminar dip," a zone of low drag on account of the laminar boundary layer. The limits of this laminar dip are not absolutely identical with the angles of incidence of constant velocity. They still are very much dependent on the Reynolds number

$$Re = \frac{U_\infty l}{\nu} = 10^6 re \qquad (2)$$

where U_∞ represents the face velocity, l the length of the profile, v the kinematic viscosity. For the sake of simplification, the Reynolds number re, reduced by 10^6, is introduced.

With smaller Reynolds numbers there generally still exists a laminar boundary layer if there is a small drop in velocity, that is, the angle of incidence has exceeded that of constant velocity. In that case, the laminar dip is larger than indicated by the angle of incidence data with constant velocities. With large Reynolds numbers, the opposite is true; a transition often occurs if a slight rise in velocity is in evidence. Then, the laminar dip is smaller than indicated by the respective constant velocity.

As a matter of principle, we designate as laminar dip that angle of incidence or c_A region in which the theoretical velocity distribution on upper and lower surface has larger stretches of nondecreasing velocity simultaneously; in the noted example, it extends from $\alpha = 3.5°$ to $\alpha = 8.5°$, or from $c_A = 0.42$ to $c_A = 1.02$.

In this case we set $\eta \neq 1$ in order to make possible an exact comparison with NACA profiles in hand for which $\eta > 1$ has also been used. The symmetrical NACA profile 66_3-0.18 has laminar lengths up to x = 0.6 on both surfaces and a laminar dip of $c_A = -0.3$. It has, therefore, a laminar dip which is exactly as wide as that of the profile in Fig. 2, but the laminar lengths are

not as long, and it has considerably greater thickness, amounting to 18%. If it were cambered in such a manner that the center of the dip, also frequently referred to as design c_A or c_{Ai}, were as high as that of the profile in Fig. 2, then the result would also be, aside from the disadvantage of greater thickness and shorter laminar lengths, one of inexact constant velocity in borderline cases. The advantage of the new method can be traced back primarily to the fact that the leading edge was exactly calculated, thereby eliminating any unnecessary effect of stagnation.

Even more distinct is the comparison with the method of E. Truckenbrodt [3]. In this instance we will not present the example given by Truckenbrodt himself, in which an airfoil has constant velocity on both sides at the same angle of incidence and has a thickness of 12%. According to the new method, a problem of this sort would result in a disappearing thickness. A different profile, calculated by F.X. Wortmann [5], has a laminar dip of $c_A = 0.63$ to $c_A = 1.13$ and a thickness of 15%. The section of velocity drop extends on the upper surface to about 40% and on the lower surface approximately to the trailing edge. The same problem was solved by the profile in Fig. 3 which has a thickness of only 9%. For the minor thickness of this profile, the velocity drop required by Wortmann is already too great. In the vicinity of the trailing edge there occur, in consequence, negative profile thicknesses or an overlapping of upper and lower surface, a fact that was already evident prior to the calculation, from the closing components both pointing upward. /250 If a profile is desired that has a thickness of 15%, as that of Wortmann, then a considerably larger laminar dip can be selected.

A profile is shown in Fig. 4 which exhibits stretches without velocity drop that are equally as long as those of Wortmann's and a thickness that is equivalent to his. In order to obtain this thickness, which is greater in comparison with the preceding profile, a considerably larger laminar dip than that of Wortmann

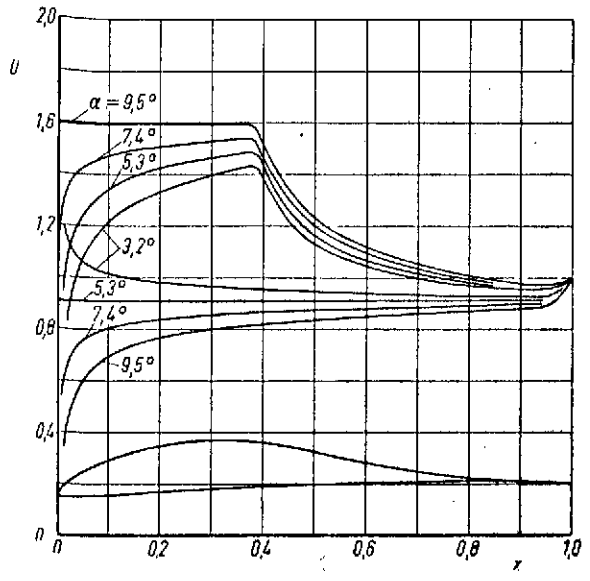

Fig. 3. Profile in accordance with FX 049-915 of Wortmann-Truckenbrodt.

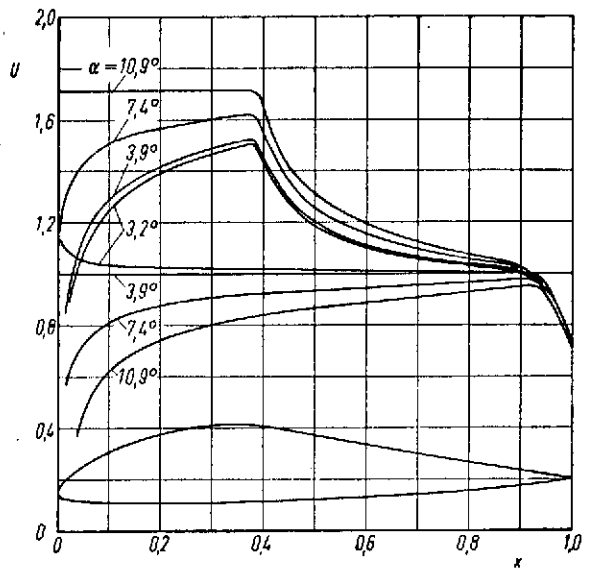

Fig. 4. Profile STF 494-915.

can be selected. It ranges from $c_A = 0.46$ to $c_A = 1.3$ and is, therefore, 70% larger than the one of Wortmann. This increase too can be traced back to an exact calculation of the leading edge.

A comparison with the findings of Lighthill can be dispensed with. If equally simple assumptions are used for velocity distributions, the same profiles are obtained except for quite insignificant differences. The advantages of Lighthill's method consist in a reduced calculating effort and in the many possibilities of assumed velocities.

3. Theory of Boundary Layers, Method of Calculation

The known methods for calculating boundary layers also left much to be desired with respect to their application to profile theory. The most satisfactory results were obtained by one-parameter methods, based in the well-known manner on the theorem of momentum and the conservation of energy. They had the disadvantage, however, of covering by means of the respective solution method only one type of

boundary layer (laminar or turbulent, with or without sucking away of the boundary layer [6, 7, 8]). It was first E. Truckenbrodt who calculated laminar and turbulent boundary layers by means of approximately the same solution method [9]. This method, which was also used by F.X. Wortmann [5], was, however, not accurate enough for turbulent boundary layers with greater pressure rise, due to the fact that some purely mathematical simplifications have too great an effect. H. Schlichting and W. Pechau [10] extended the range of the procedure so that the case with suction was included.

In September 1958, at the Third European Aeronautics Convention in Brussels, a paper was read on the calculating method for the case without suction [11]. A detailed publication on a calculation of boundary layers with suction is in preparation. We will, therefore, refer here only to attainable results. The calculating effort for the method that had originally been prepared for manually operated calculators is comparable with that of the simplest method. The method is well suited for programming on digital computers, so that large-scale calculations can be carried out.

In the following, all lengths of profile length l (x, y, momentum loss thickness, energy loss thickness) and all velocities with U_∞ have been made dimensionless.

For a given velocity distrubtion U(x) and a Reynolds number in accordance with (2), we now calculate the momentum loss thickness in the boundary layer for velocity u(x,y), as follows:

$$\vartheta(x) = \int_0^\infty \frac{u(x,y)}{U(x)}\left[1 - \frac{u(x,y)}{U(x)}\right] dy \tag{3}$$

and the energy thickness form parameter as follows:

$$\bar{H} = \frac{\delta^{**}}{\vartheta} \tag{4}$$

where the thickness of energy loss is defined analogous to (3) by

$$\delta^{**} = \int_0^\infty \frac{u}{\bar{u}}\left[1 - \left(\frac{u}{\bar{u}}\right)^2\right] dy \qquad (5)$$

Form parameter $\bar{H}$ offers indications for the burbling tendency of the boundary layer. The greater $\bar{H}$, the farther we are away from burbling. By and large, the data compiled in Table 1 hold true.

TABLE 1. VALUES OF $\bar{H}$ IN VARIOUS SPECIAL CASES.

Boundary layer	Laminar	Turbulent
Asymptotic suction	1.6667	
Stagnation point	1.6171	
Flat plate	1.5682	1.71 to 1.75
Burbling	1.5184	1.46 to 1.58

The values for individual special cases in the boundary layer are unequivocal on account of simpler conditions and a basic one-parameter character, whereas for the turbulent boundary layer they depend on the Reynolds number. A special uncertainty resides in the turbulent separation, with which we will deal in detail later.

Possibly at the trailing edge of a flat plate or a profile, at the conclusion of a boundary layer calculation, the amount of drag can be calculated by means of the thickness of momentum loss and the form parameter in accordance with Squire-Young, in the following manner:

$$c_{tW} = 2\vartheta U_1^{\frac{H+5}{2}} \qquad (6)$$

if U_1 is the velocity at the end (made dimensionless with U_∞) and H the form parameter $H = \delta^*/\theta$, which has been assumed as unequivocally dependent on $\bar{H}$ for the laminar as well as for the turbulent

case. The so-called displacement thickness δ^* of the boundary layer is defined by /251

$$\delta^* = \int_0^\infty \left(1 - \frac{u}{U}\right) dy \tag{7}$$

Figure 5 represents a comparison between the new theory and computations by Truckenbrodt and experiments by Wortmann. The possible magnitude of the pressure rise calculated by Truckenbrodt proved too great when checked experimentally. There appeared phenomena of burbling that can be traced back to an increase in thickness of momentum loss that had not been adequately dealt with. The plotted boundary layer thicknesses measured by Wortmann are in accordance with the velocity curve of Fig. 5. Whereas the values calculated by means of the new method show good approximation to the experiments, the theoretical values of Truckenbrodt are considerably lower.

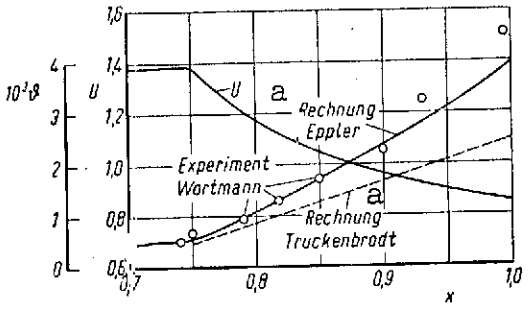

Fig. 5. Boundary layer theory, calculation of example and comparison with experiment.

Key: a. Calculation

Figure 6 shows several experimental velocity distributions where separation had occurred as well as the form parameter values that had been calculated for them. Predicting the location of a separation is still one of the specially difficult features of calculating turbulent boundary layers. All three of the velocity distributions that were used resulted in a separation of the turbulent boundary layer. Theoretically, this separation is determined by a drop of the form parameter below a certain value at which the wall shear stress practically vanishes. While the assumption to date had been that the turbulent boundary layer

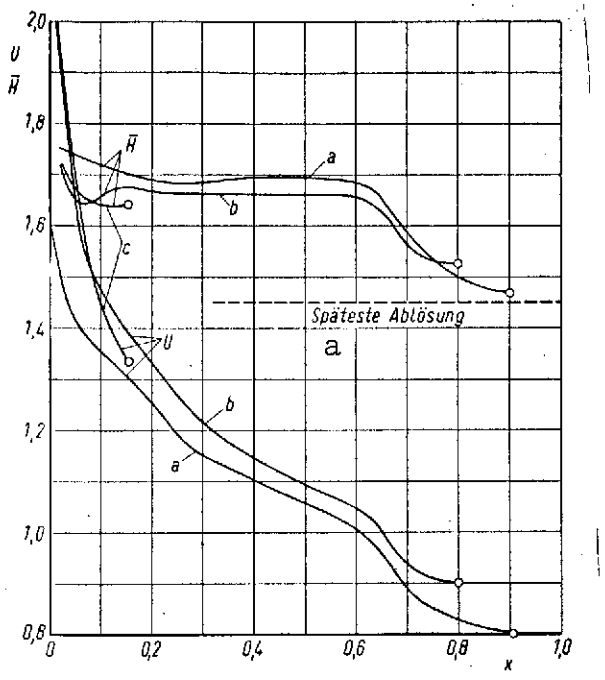

Fig. 6. Recalculation of separated experimental boundary layers.

Key: a. Latest separation

would not adhere until the wall shear stress vanishes, on calculating the experiments subsequently, it was found that the limit for separation is nearly reached. Lately, attention has been called to the effect of dead water [12]. According to this view, a connection between the tendency of the boundary layer to adhere longer to the airfoil and smaller values of the separation parameter sound quite plausible; this tendency is evident in Fig. 6. It can be assumed that the beginning of turbulent separation, unless it happens quite suddenly, occurs at relatively low form parameter values. For the time being, it is not possible to apply more than this rough criterion. However, it already allows us to fix velocity distributions in such a manner that a turbulent separation can be avoided with certainty.

4. The Mathematical Model

By means of the noted methods of calculation for the theory of boundary layers and airplane wings, it is possible not only to design profiles with specified characteristics of pressure distribution, but also to compute subsequently many data for the resulting profiles that had hitherto been determined only in the wind tunnel. This pertains mainly to boundary layer data, instability of the laminar boundary layer, and drag at different angles of incidence and Reynolds numbers. It is thus possible to calculate complete polar diagrams, to compare the results of different profiles with each other and -- just as by means of

wind tunnel tests -- select from systematically modified series of profiles those that are best suited for a certain purpose.

However, it is necessary always to keep in mind that all comparisons are only on the basis of a purely mathematical contrivance consisting of formulas, that has lately been designated as a "mathematical model" of certain natural events. The mathematical model, no more than a "model test," possibly in a wind tunnel, cannot cover everything that takes place during the use of an airfoil on an airplane. Whereas, for instance, the mathematical model does not account for three-dimensional events, in the wind tunnel there also occur secondary currents other than at the airplane wing. Neither wind tunnel results nor theoretical findings are likely to be blindly applied to an airplane wing; however, it should be possible to draw certain conclusions for actual wings from experiments as well as from theoretical comparisons.

The fact that lately mathematical models are again moving more into the foreground is connected with the possibilities presented by digital computers that permit the use of a foundation of more complicated and more reliable systems of formulas. In addition, the application of the mathematical model is frequently cheaper than the experiment. The latter fact counts for much, especially for the combined application of boundary layer and profile theory under discussion here. /252

In the following, we will demonstrate how the noted mathematical model can be applied. No comparisons with nature have yet been drawn, although only by their use can the usefulness of the model be proven and possibly an improvement in the formula setup be found. Our aim, first of all, is to explain the range of the formula setup by means of some examples and to show the possibilities that offer themselves if the road that we have taken continues to be practicable.

5. Applications

5.1. Optimal Form of Pressure Rise in Turbulent Boundary Layer

Whereas we know with certainty that in the laminar boundary layer the greatest possible pressure rise is attained if the borderline of burbling is approached as close as possible with the form parameter, we are by no means as certain with regard to the turbulent boundary layer. However, even there some information can be expected regarding the still possible pressure rises if the tendency to separation or the form parameter value is kept constant. These boundary layers, which erroneously have often been designated, just as in the laminar case, as "similar boundary layers," have been obtained with relative ease by means of the present programs for profile calculations by varying the velocity drop during step-by-step integration until the form parameter remained constant. Some of the results are presented in the following graphs. In accordance with the given form parameter values, basically different patterns of velocity, beginning with U = 1, will naturally result.

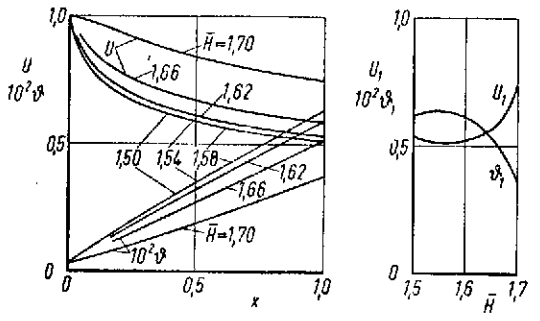

Fig. 7. Similar turbulent boundary layers.

In Fig. 7, starting at a thickness of momentum loss of θ_o = 0.0003, the course taken by U(x) and θ(x) has been shown for different form parameter values. The Reynolds number, set at re = 1, was derived from the initial velocity and the unit of length. The relatively small velocity drop depicted results from $\bar{H}$ = 1.7. A small decrease in the form parameter in the direction of burbling results in a considerably greater velocity drop with $\bar{H}$ = 1.66. The fact is remarkable that a further decrease in form parameter, which would

not reach the borderline of separation before $\overline{H} = 1.46$, does not result in any considerable increase in the possible drop in velocity.

Due to the fact that in Fig. 7 the curves lie very close together, the course taken by the final value U_1 and θ_1 at $x = 1$ plotted against form parameter $\overline{H}$ is at the right-hand side of the figure. Especially conspicuous is the fact that the lowest final velocity value is not reached when approaching quite close to the burbling point, but considerably sooner, at about $\overline{H} = 1.58$. This finding has been established throughout all calculations of similar boundary layers.

The velocity curve exhibits the familiar picture that at first the velocity drop is large, but subsequently gets smaller and smaller. The thicker the boundary layer, the less it can tolerate a velocity drop without a separation occurring.

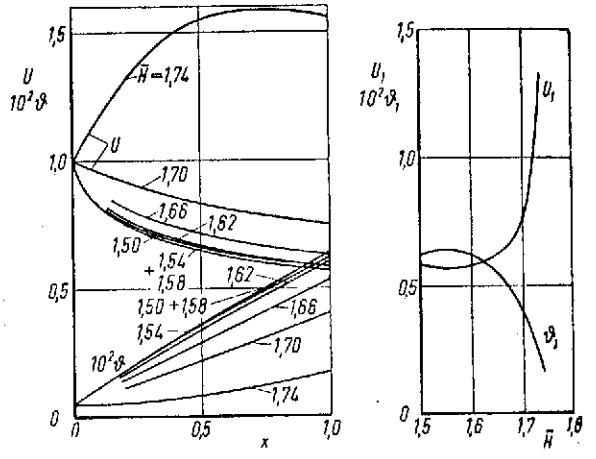

Fig. 8. Similar turbulent boundary layers.

This is also clearly visible in Fig. 8, where the same calculation for the same Reynolds number with a different initial value of momentum loss thickness, $\theta_o = 0.0005$, has been presented. The velocity drop that can be attained, which is shown to the right in the figure, is in this case considerably smaller than in the preceding example. It should be noted that the maximum velocity gradient was again reached at approximately $\overline{H} = 1.58$.

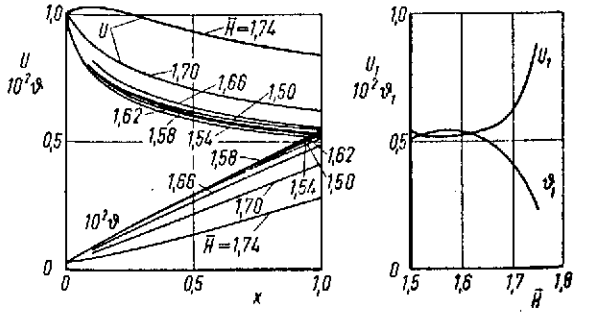

Fig. 9. Similar turbulent boundary layers.

Of interest, furthermore, is the effect of a change in the Reynolds number. In Fig. 9, as in Fig. 7, the thickness of the momentum loss is θ_o = = 0.0003, but it is based on four times the Reynolds number, re = 4. With an increasing Re number, a higher possible velocity gradient is expected. Oddly enough, this does not happen if the initial value θ_o is maintained. There is, rather, practically the same value of the lowest final velocity as in Fig. 7. The form parameter value /253 that results in the largest velocity gradient is insignificantly smaller than before. In this case also, the attainable velocity drop is not as great when approaching close to the border where separation takes place than it is shortly before that line is reached.

The question is important why there is here no confirmation of the generally known tendency of larger possibile velocity gradients with larger Reynolds numbers. This is due to the fact that the initial value of the momentum loss thickness has been kept constant. There are generally smaller momentum loss thicknesses for a high Reynolds number. Consequently, the momentum loss thickness that was kept constant signifies that relatively higher initial momentum loss thicknesses had been selected for higher Reynolds numbers.

In order to study more in detail the phenomenon that the possible velocity gradient changes little with the Reynolds number at a constant initial value of the momentum loss thickness, a large number of similar boundary layers, each with the form parameter $\bar{H}$ = 1.58, which leads approximately to the maximum velocity

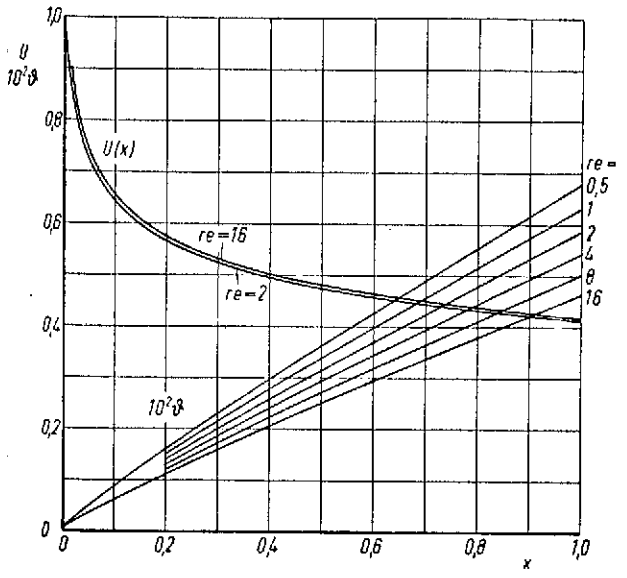

Fig. 10. Borderline case of similar boundary layers.

gradient, were calculated all the way through. In Fig. 10 are plotted the resultant curves of velocity and momentum loss thickness for an initial value of θ_o = 0.0001 and six Reynolds numbers of re = = 0.5 to 16.

Whereas the lines for the momentum loss thickness stand out clearly, it was not possible to plot all the lines for the velocity distribution, as they are located too close together.

Although, in principle, it would be possible to calculate the similar boundary layer and the possible velocity gradient for each combination of initial values, the already acquired relationship is adequate for a good assessment of possibilities. Wherever the momentum loss thickness θ_o determines practically all by itself the possible course taken by velocity, then it is possible to find readily in Fig. 10 the initial value of the momentum loss thickness at the respective Reynolds number and, on the basis of the corresponding values of x_o and U_o, to locate immediately the possible further course of velocity. It must of course be proportionally extended to the respective value of the velocity of the problem, taking into account the change of Reynolds number.

Even a further simplification is justified. It is not even necessary to consider the different course taken by the momentum loss thickness at different Reynolds numbers, but it is possible to pick out a single one of these lines, possibly the one with

re = 4. If now, for an initial value of θ_o which belongs to a different Reynolds number, x_o is located by means of this picked-out line, then a considerable error results for U_o. However, if the adjacent velocity curve is distorted to the given initial value of velocity, the error is corrected to a large degree.

If the following exponential law were to hold true for the velocity curves

$$U = Ae^{-Bx} \text{ or } U'/U = \text{const}$$

then the correction would be complete. In an actual case, U'/U would decrease, but not to the extent that the restriction to a single θ line would result in an important error. Figure 11 depicts the same diagram as Fig. 10, but for a greater initial value of the momentum loss thickness of $\theta_o = 0.0005$. Here, the lines of velocity already differ more but are still close enough together. The errors that can be made by a restriction to a single θ line also lie in the order of magnitude of this difference. Until now, it has been possible to put up with it without difficulties. In each case, it would be possible to arrive at more exact values from the diagram in Fig. 10 by taking into account the Reynolds numbers when locating the initial value of θ.

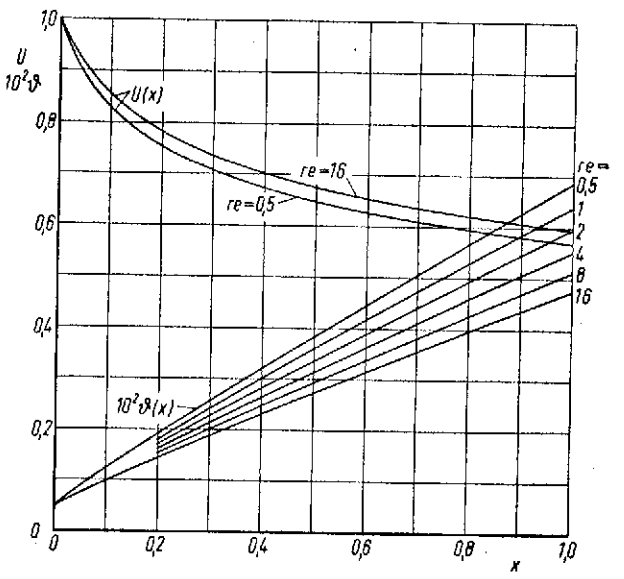

Fig. 11. Borderline case of similar boundary layers.

The start of the turbulent boundary layer is usually connected with a small boundary layer thickness. In order to facilitate the locating of corresponding θ and U values, the beginning of the

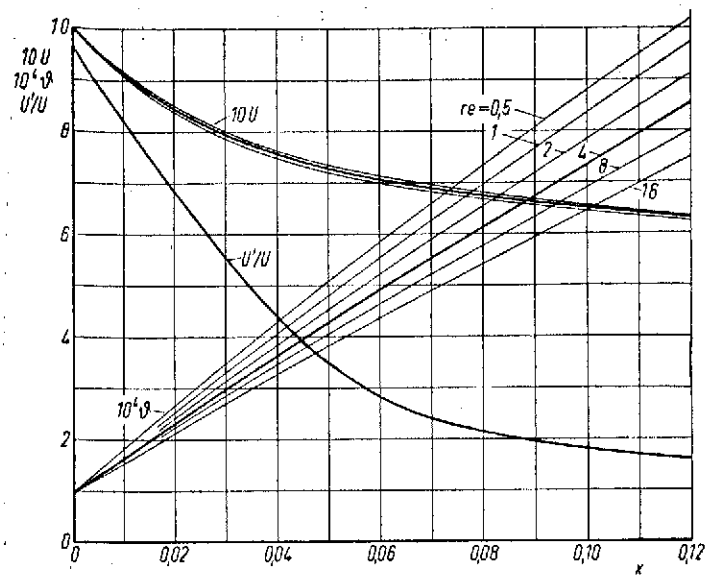

Fig. 12. Borderline case of similar boundary layers, enlarged representation of initial region.

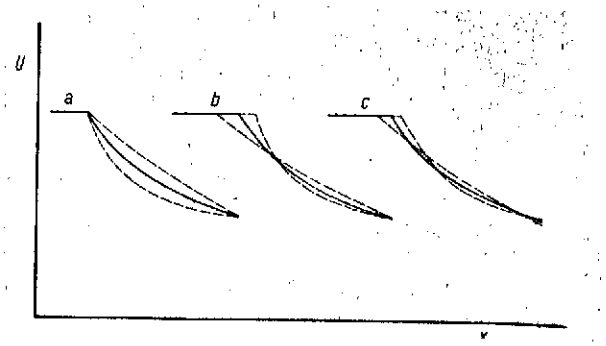

Fig. 13. Comparable forms of velocity drop.

diagram in Fig. 12 has been enlarged. There, a line U'/U has also been plotted. This quantity is used to special advantage in the profile theory during introduction of velocity distribution.

The diagrams as /254 shown offer a simple method for finding velocity distributions for given initial thicknesses of momentum loss that are liable to result in a constant form parameter and certainly not in a turbulent separation. However, it is still completely unclear whether these represent the most favorable course that velocities can take, especially in view of an application for airfoils. It might be possible that forms of pressure rise in which the form parameter approaches the borderline of separation only gradully would permit a greater pressure rise. In addition, it is necessary to investigate which points of view become decisive; it is not only of importance that there is no separation at the profile, but also to attain minimum drag at these conditions. We cannot, therefore, avoid investigating, by using concrete examples of airfoils, the effect of different

courses taken by velocity. It will be possible to use data gained from "similar" solutions as points of reference and, above all, to draw on adjacent forms for comparison. The boundary layer theory by itself, however, will not be adequate for reaching a decision.

A comparison of different shapes is carried out on the upper surface of profiles that are in accordance with the problem of the simple laminar airfoil. The original profile is shown in Fig. 14b. Its laminar dip extends from $\alpha = 4.5°$ to $\alpha = 13.2°$, i.e., approximately from $c_A = 0.5$ to $c_A = 1.45$. The laminar lengths on the upper surface are $x_{1o} = 0.34$, on the lower surface, $x_{1u} = 0.8$. The form of the velocity drop on the upper surface was arrived at by first calculating (on another profile, on which all data were the same, but the velocity drop had been estimated) the momentum loss thickness θ_o at the beginning of the pressure rise for $re = 1$ and $\alpha = 13.2°$. Subsequently, from Figs. 11 and 12, the velocity distribution was determined that exactly corresponded to the conditions of greatest velocity drop at constant form parameter that prevailed there. The profile depicted in Fig. 14b was calculated by means of this form. A calculation based on the boundary layer theory showed that during conversion from estimated to final form of the velocity rise, the quantity θ_o remained intact accurately enough and that the form parameter in the pressure rise region yielded the assumed values. /255

In order to study the significance in the profile theory of a form of velocity determined in this manner, it is possible to calculate "neighboring" profiles which, however, must be selected with some caution. To begin with, it might be considered, possibly in accordance with Fig. 13a, to leave unchanged the beginning of the pressure rise and its total height and to vary the steepness at the beginning. While this does supply some information, it does not as yet represent the correct method for

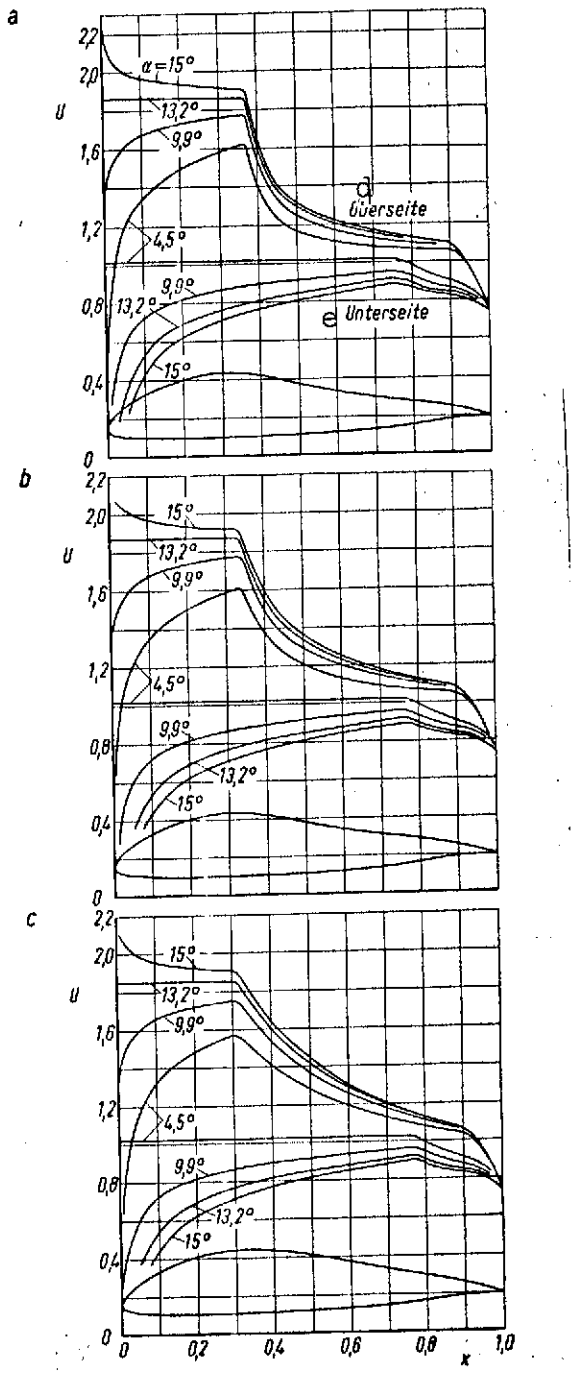

Fig. 14. Three comparison profiles with equally full trailing edge and equal laminar dip limits.

Key: a. Velocity drop initially steeper than in borderline case of similar boundary layers

[Key continued on following page.]

comparisons. In comparing such profiles with each other, the following is observed:

1. The too-steep pressure rise quickly results in separations. This is not a foregone conclusion, due to the fact that the value of the form parameter at the beginning is still a long way from separation. However, its initial value has little effect compared to that of momentum loss thickness.

2. The too-flat pressure rise does not as yet result in separation and also yields the same value of momentum loss thickness at the end of the pressure rise. Therefore, if at the beginning of the pressure rise the steepness that is possible is not fully utilized, no disadvantage results with respect to the boundary layer theory.

3. The profile with the pressure rise that is initially steeper has a considerably

Key to Fig. 14, cont'd:

b. Equally steep
c. Flatter
d. Upper surface
e. Lower surface

more pointed trailing edge; the one that is initially flatter has a considerably fuller trailing edge. This results from the fact that the share contributed by a velocity drop to the closure of the profile is calculated by means of an integral (compare [5]).

The fact noted under point 3 condemned the comparison as it had been carried out. The differently full trailing edges require differently large closing components in the distribution of pressure. They, in turn, occasion differently large separations in the vicinity of the trailing edge, the effect of which on drag is not covered in the theory of boundary layers. Although such separations occur in practice on all profiles, a reliable comparison within the framework of the theories presented here is obtained only if the trailing edges have the same fullness in each case or if the closing components in the distribution of pressure are equally large.

The example that we have discussed shows that the theory of boundary layers would permit without drawback a pressure rise for which the initially possible pressure rise has not been fully utilized, but that in this case disadvantages with regard to the theory of profiles would occur. Since the tendency is to resort to flatter pressure rises on account of the laminar bubbles during burbling that occur at the beginning of the pressure rise in proportion to its steepness, it is important to assess the magnitude of the disadvantages connected with it. For this reason, the temptation is to carry out the comparison in the manner shown in Fig. 13b by again keeping the total height of the pressure rise constant and starting with the initially flatter pressure rise

sooner, by so much that the closing components will remain unchanged, while the initially steeper one is begun correspondingly later. However, this type of comparison is not conclusive either. An earlier beginning of pressure rise requires a smaller value of θ_o; according to Figs. 10 and 12, the total height of the pressure rise can be greater if in each case the form of rise as determined there is chosen. Since we always wish to compare with this form, we must base the calculation of the comparison profiles on the principle sketched out in Fig. 13c. In this case also the initially less steep pressure rise is used sooner; however, its total height is fixed higher corresponding to the smaller θ_o; the reverse holds true for the initially very steep pressure rise. This results in the displacement of the beginning of pressure rise not being as great as that of the comparison principle of Fig. 13b.

Some preliminary calculations with estimated θ_o values were still necessary for determining θ_o in order to arrive at a final determination of the comparison profiles depicted in Figs. 14 a and c. The depicted comparison profiles meet all requirements. Especially the limits of laminar dips, the beginning of pressure rise at the lower surface and the fullness of the trailing edge are exactly the same. The size of the pressure drop at the upper surface is determined for the θ_o values at re = 1 and $\alpha = 13.2°$ from Figs. 11 and 12; only the initial steepness in the case of c is smaller, and in the case of a, it is bigger than would have resulted from the diagrams.

A large number of calculations for boundary layers and drag has been made for these three profiles. A selection of typical findings is presented in Fig. 15. Of greatest interest, first of all, is naturally the angle of incidence $\alpha = 13.2°$ -- or in accordance with (1), the coefficient of lift $c_A = 1.45$ -- at re = 1; this is the case on which the comparison was built. It is evident

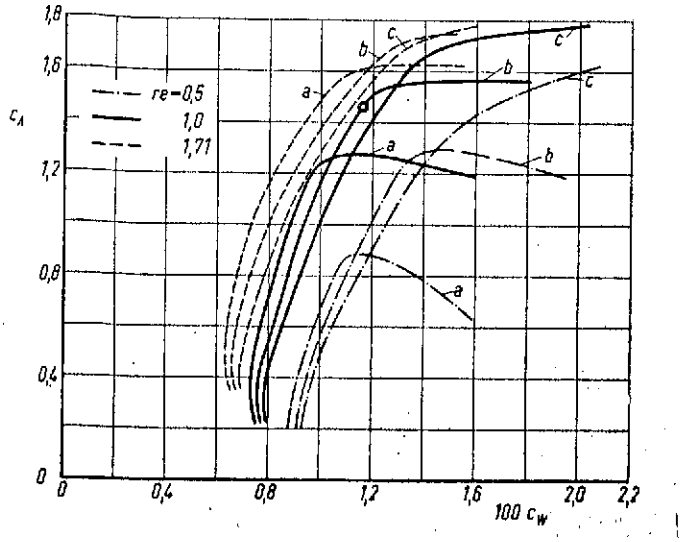

Fig. 15. Calculated polar curves of comparison profiles of Fig. 14.

that in this case profile b is the most favorable. Profile c, as expected, has no greater separations than b, due to laminar lengths that are shorter for purely theoretical reasons regarding the profile, but it possesses somewhat more drag. Profile a exhibits premature separation. It even occurs very suddenly. In any case, for this reason a too-steep velocity drop must be avoided. The flatter velocity drop entails the advantage, as against the somewhat greater amount of drag, of effecting a very slow separation from the direction of the trailing edge. This is indicated in Fig. 15 by the fact that the polar curve still shows some upward slope at the onset of separation in the vicinity of $c_A = 1.45$, that the increase in drag is, therefore, still connected with an increase in lift.

For the comparison of profiles, calculations of drag at other Reynolds numbers will also be used, as these vary anyway for the /256 wing and for individual flight conditions. A reduction of the Reynolds number to re = 0.5 shows the same picture at the lower part of the polar curve. On this occasion, where the rise in pressure has anyway not been fully utilized, the too-steep pressure rise results in the smallest amount of drag. However, separation occurs here still sooner and still more suddenly. At the profile, which is exactly right for re = 1, at the smaller Reynolds number, separation also occurs too soon and too suddenly. At a flatter pressure rise, separation also occurs already before reaching the limiting angle of incidence for which the calculation takes place. However, it is still very weak and progresses only slowly.

At an increased Reynolds number the profile with the too-steep pressure rise exhibits no separation up to the limiting angle of incidence; shortly thereafter, however, it occurs again rather suddenly. The two other profiles, with almost no exception, exhibit more drag but a better behavior relative to separation.

All in all, the conclusion can be drawn from Fig. 15 that we come close to the optimum if the form of velocity drop is taken from the diagram of similar boundary layers for the one respectively selected. However, attention will always have to be paid to keeping the initial steepness of the velocity drop small enough, because in that way the separation attitude is improved. Another reason for a less steep velocity drop, especially at smaller Reynolds numbers, is to be found in the occurrence of laminar bubbles during burbling.

From the preceding examples it is evident that the velocity curves derived from the "similar" solutions for the turbulent boundary layer come very close to the drag minimum that can be attained. It is true that adjacent curves with smaller initial gradients are better from the standpoint of boundary layer theory, but they exhibit disadvantages from the standpoint of profile theory. There are simple diagrams for obtaining an individual course. The decision will have to be made in each individual case whether a more harmless separation attitude and a more advantageous change in boundary layer should be attained at the expense of drag.

5.2. Distribution of Laminar and Turbulent Sections on Upper and Lower Surface

Soon after the first development of laminar profiles, it became evident that the distribution of laminar sections on the upper and the lower surface has a considerable effect on the moment coefficient of the ensuing airfoil problems.

F.X. Wortmann [2] determined in addition that the drag coefficient is also affected by it. However, when assessing his findings, it must be noted that the selected approximations play an appreciable role both in the boundary layer theory and in the profile theory. Above all, in Wortmann's method of approximation for calculating the profile at the trailing edge of the upper and lower surface, the velocity is not the same. In any case, the equalization of pressure that always exists in an actual case seems to take effect to a greater extent than originally anticipated.

When comparing profiles that have different laminar lengths on upper and lower surface, care must be taken that the trailing edge is equally full in each case and, in addition, see to it that the velocity drop depends on the momentum loss thickness at the transition point.

A simple laminar profile is again chosen to serve as a problem on which to carry out the comparison. The laminar dip extends from $\alpha = 4.5°$ to $\alpha = 13.2°$. The length x_{lu} of constant velocity on the lower surface is varied, starting from very small values around 0.05 to close to the trailing edge at 0.95. The momentum loss thickness θ_o at the transition point on the lower surface is calculated in each case for re = 1.71 and subsequently the form of the pressure rise is determined in accordance with Figs. 10 and 12. On the upper surface, as a matter of principle, the boundary layer thickness at the transition point is also calculated for the selected starting length x_{lu}, but for an $\alpha = 13.2°$ and a smaller Reynolds number, namely, re = 1; then we proceed the same way as on the lower surface. The different Reynolds numbers are due to the fact that on an airplane the higher lift coefficient is reached at a lower speed. For a given laminar length on the lower surface,the one on the upper surface is found by the requirement for having the same overall fullness at the trailing edge. In order to meet all of these requirements, iterations were

occasionally necessary when profiles resulted that were based on an initially estimated momentum loss thickness at the transition point, and where the subsequently calculated momentum loss thickness turned out to be different from the estimated one. However, it was possible largely to avoid iterations by means of skillful interpolations.

The series of profiles that came into being under the noted conditions are shown in Fig. 16. This series exhibits some surprising features. Generally, the expectation would be that for the same fullness of trailing edge, a longer laminar section x_{lu} on the lower surface would demand a shorter x_{lo} on the upper surface. On the whole, this tendency is exhibited by the series; however, at the beginning, it is seen that increases of x_{lu} from 0.01 to 0.1 do not entail any reduction of x_{lo}. Also to be observed in the region of very large x_{lu} is a heavy drop of x_{lo}. Consequently, it does not look like a good policy to demand laminar sections on the lower surface that are too long, as it is only possible to obtain them by means of a greater shortening on the upper surface. This shows that a relatively short region of declining velocity already contributes much to the closing of the profile, a fact that can also be substantiated by means of the profile theory.

For this profile series we also carried out a very large number of boundary layer and drag calculations. Part of the findings are depicted in Fig. 17. First of all, we want to mention the dependence of a possible laminar length on the upper surface on that of the lower surface. In addition, the moment coefficient c_{Mo} for it has been plotted at zero lift, which of course is very large for extreme profiles of higher camber and which decreases with increasing laminar length on the lower surface. In addition, the thickness of the resulting profiles is noted, profiles which reach their maximum where x_{lu} is slightly larger than x_{lo}. However, essential

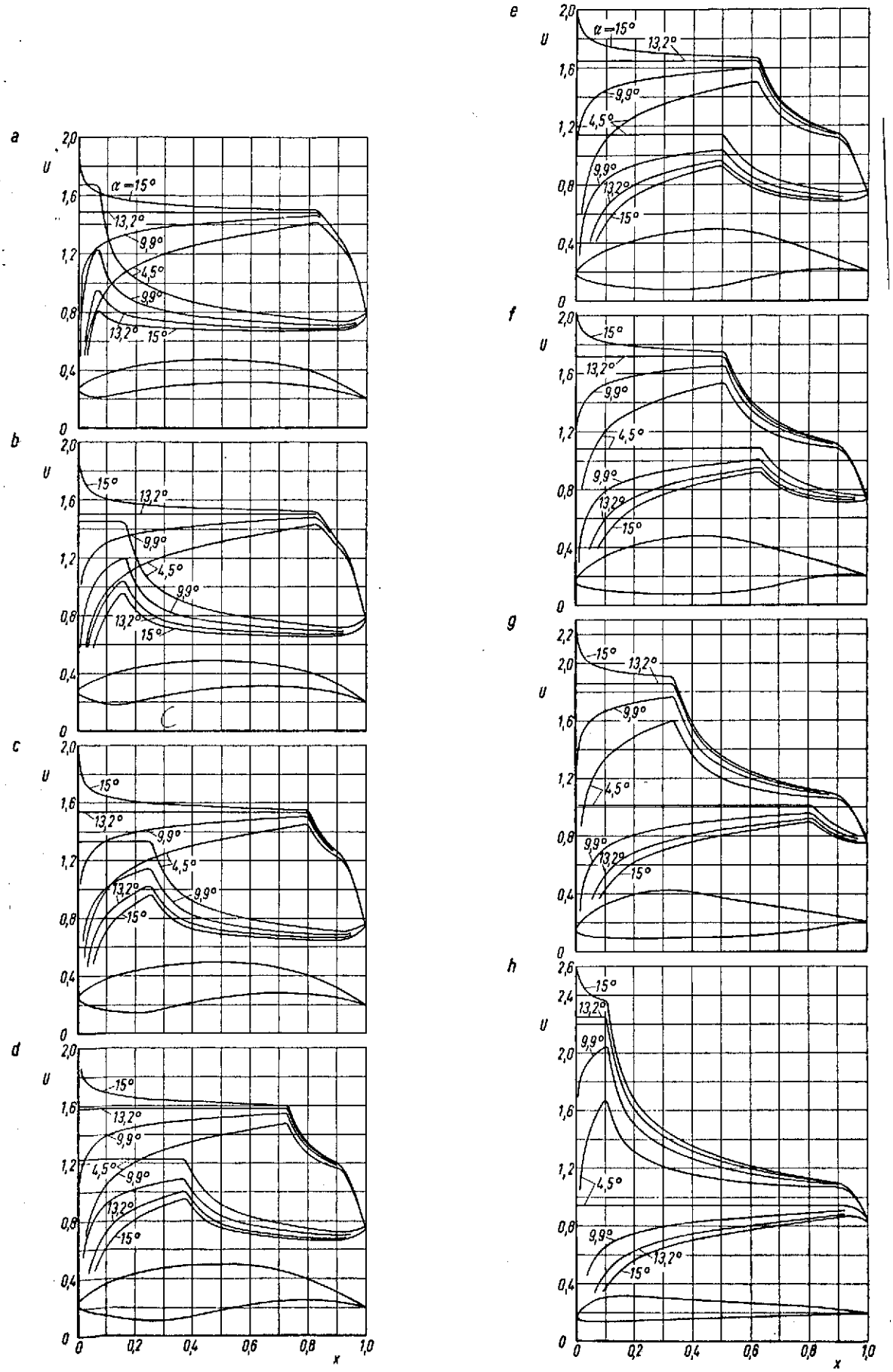

Fig. 16. Profile series with different distribution of laminar lengths x_{lo} and x_{lu} on upper and lower surface with laminar dip limits maintained and constant trailing edge.

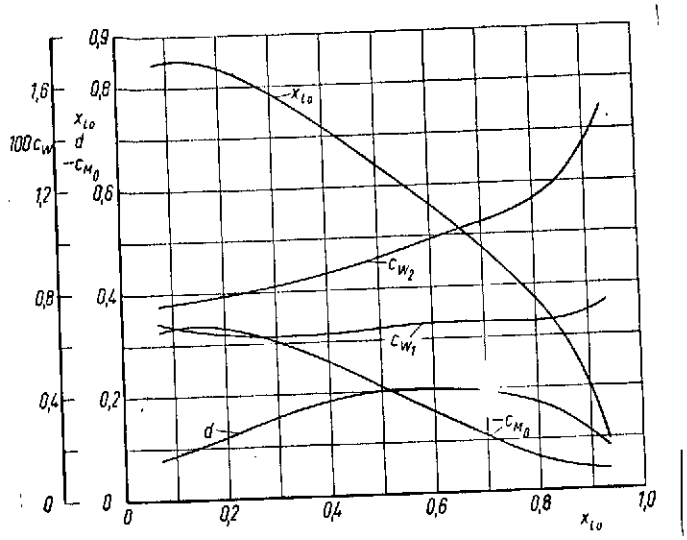

Fig. 17. Characteristic quantities of profile series of Fig. 16.

for selecting the most favorable profile are the drag coefficients. In this instance, we specified the two characteristic values, namely, the drag coefficient c_{w2} at the large angle of incidence $\alpha = 13.2°$ and the small Reynolds number re = 1, and additionally that of c_{w1} at the small angle of incidence $\alpha =$ /257 /258 $= 4.5°$ and the large Reynolds number re = 1.71. It turns out that the value of c_{w1} hardly changes at all. In contrast, c_{w2} increases with increasing laminar length on the lower surface. This result is contrary to Wortmann's conception. He allots considerable advantage to the extreme cases of long starting distance on lower and upper surface. In this instance, we find that in extreme cases the loss of closure component in accordance with profile theory that had not been determined exactly by Wortmann, exceeded the gain in accordance with boundary layer theory. With large lift coefficients, that is, high average flow velocities on the upper surface, a lengthening of the laminar boundary layer on the upper surface has a greater effect than the corresponding shortening on the lower surface. With small coefficients of lift, however, it does not matter how the laminar lengths are distributed. In that case, the profiles where the laminar length is approximately equal on upper and lower surface are superior on account of their greater thickness.

Consequently, if the interest is along the lines of little drag at a small amount of lift, the choice of profile will be in the direction of the small c_M values, whereas in those cases where drag coefficients that are still favorable at high coefficients

of drag are to be attained, the larger c_{Mo} will have to be put up with.

5.3. Limited Moment Coefficient

For structural reasons, in many cases the demand is made on the airfoil that the moment coefficient must be limited. As can readily be seen in Fig. 17, this restricts the choice of a profile to a considerable extent. In case the moment coefficient must be kept small, profiles with long laminar sections on the upper surface are out of the question. Consequently, small drag coefficients with large lift coefficients are also out of reach. Furthermore, the fact must be recognized that it is basically not possible to attain arbitrarily small moment coefficients for given limits of laminar dips if we are unwilling to put up with boundary layer separations. For instance, a profile with fixed aerodynamic center with vanishing moment coefficient c_{Mo} cannot be attained with the limits for laminar dips that have been assumed for the profile series noted. For this, the laminar dip must be moved downward. This results in a reduction of maximum lift. Since, in addition, small moment coefficients at the lower surface always require longer laminar distances than on the upper surface, which increases drag at larger coefficients of lift, it can in general be established that placing a limit on the coefficient of drag will result in a considerable restriction of attainable profile characteristics at large coefficients of lift. For flying-wing aircraft, the attainable maximum lift is, therefore, generally within bounds; for other planes, where the limiting of a moment coefficient is necessary for reasons of physical properties and danger of flutter, it will be advisable to use flaps for the purpose of increasing maximum lift. More exact calculation of the possible borderline cases is extensive for the general case due to the fact that the respective Reynolds number also enters into it. However, it is easily possible to determine the attainable values from case to case.

5.4. Profiles with Strong Maximum Lift

Although, especially with respect to maximum lift, calculation of the boundary layer cannot as yet furnish any exact information, a consideration of some general characteristics of boundary layer distribution will result in a certain delimiting of possibilities to attain strong lift. Besides the method of deciding on an upper limit to the laminar dip that is so high that large enough coefficients of lift can already be obtained below it, there is still another possibility that F.X. Wortmann [2] has already pointed out. If we manage to select the laminar length x_{lo} on the upper surface so large that there remains only a short region of pressure rise following maximum velocity, then above the laminar dip the distribution of velocity is such that even with a transition occurring at the leading edge, there is no danger of turbulent separation over a large range of angles of incidence at any great distance from the trailing edge.

An example of such a profile is the one already shown in Fig. 2. The velocity distribution has been plotted there for two angles of incidence above the laminar dip. It can easily be calculated that even for the larger of the two values, a separation of the turbulent boundary layer occurs only a short distance ahead of the trailing edge. The laminar dip in this case extends only over a relatively small area; however, frequently such an area is entirely adequate, especially in the case of airplanes with small aspect ratio. In those cases the induced drag at higher coefficients of lift is anyway many times as great as the parasitic drag. It is true that in the profile noted the leading edge is quite pointed, so that outside of the laminar dip high velocity peaks set in quickly, which will then, in turn, lead to separation.

Figure 18 depicts another design of a profile. In this case, the laminar dip that was selected is even smaller, which is

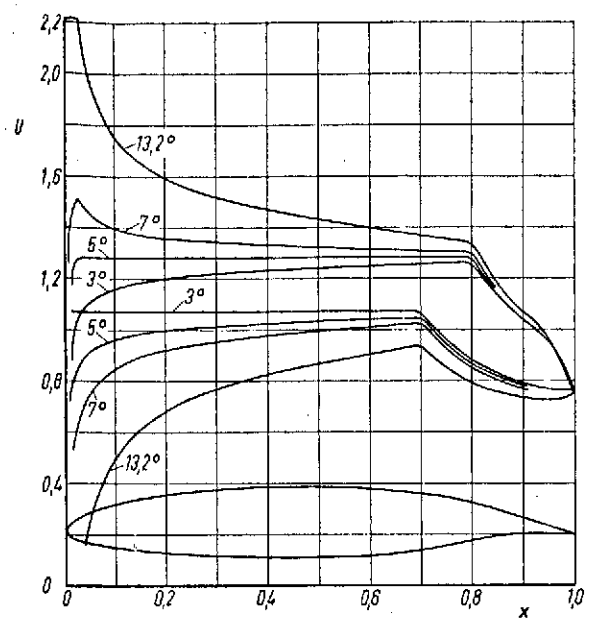

Fig. 18. Profile STE 971-514 with small laminar dip and strong maximum lift.

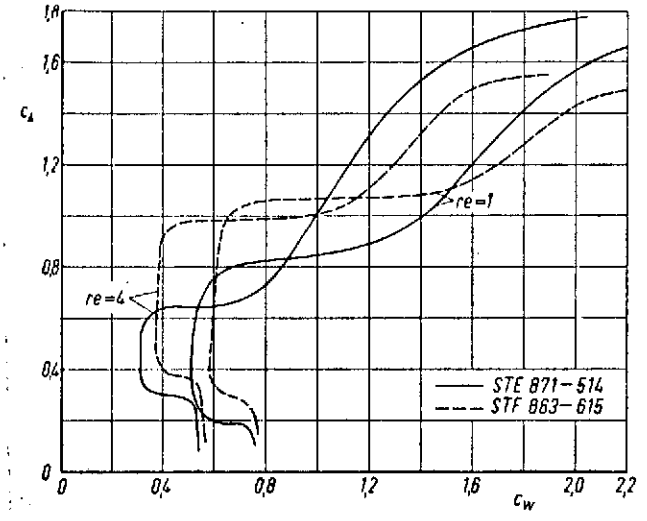

Fig. 19. Calculated polar curves of profiles STF 863-615 and STE 971-514.

frequently adequate for practical problems. Consequently, it was possible to introduce an additional section of constant velocity on the upper surface at a high angle of incidence. This increases the thickness of the profile and, above all, makes the leading edge considerably fuller than would be in conformity with the small laminar dip; the high collecting points at the leading edge are avoided. In addition, this type of profile, in contrast to the customary laminar airfoils, allows for still larger laminar distances. Therefore, the gain derived from a reduction in the size of the laminar dip results, on the one hand, in higher lift coefficients; on the other hand, in longer laminar /259 sections. The calculations of drag for the last two profiles have been plotted in Fig. 19. Even for the specified velocity distribution at the high angle of incidence of 12.5°, the danger of separation on the upper surface is a long way off. The fuller nose

resulted in a greater maximum lift and the longer laminar sections brought about reduced drag within the laminar dip; its width, however, has become smaller. These possibilities, too, since they are based on the assumption of long laminar sections on the upper surface, cannot be attained with small moment coefficients. Nevertheless, it will pay to include such profile types in design considerations of many problems, especially when modern types of construction with plastic materials come into being.

6. Results to Date

Although theory was meant to be in the foreground of the present study, we will give a brief account of the practical results that we have achieved so far. The first application of an airfoil, somewhat similar to that in Fig. 1, was in the FS 24 Phönix sailplane, prior to the time that any wind tunnel data were available. The wind tunnel tests subsequently carried out [13] and the actual results [14] were decidedly gratifying.

This initial success was followed by several calculations of profiles that were primarily meant for wind tunnel experiments and where an attempt was made to determine an optimal pressure rise by means of older boundary layer methods. The corresponding measurements, which also caused certain difficulties in the wind tunnel itself, demonstrated that the theoretical fundamentals of boundary layers urgently needed improving [15, 16]. It is not possible at present to report on the measurements or the practical application of profiles that have been calculated by means of the new boundary layer calculation method. However, the control experiments are being prepared. If they turn out positive, then not only single profiles but an entire methodology for the calculation of profiles will have been obtained, the value of which will far exceed that of an airfoil catalog.

7. Appendix: Coordinates of Several Profiles

TABLE 1. PROFILE STE 87(-3)-914 (Fig. 1).

100 x	100 y	100 x	100 y	100 x	100 y
100,000	0,000	29,582	11,019	16,989	−3,569
99,635	0,122	25,240	10,632	21,083	−3,584
98,596	0,518	21,155	10,133	25,556	−3,521
97,007	1,202	17,373	9,523	30,345	−3,396
94,983	2,120	13,941	8,796	35,385	−3,224
92,596	3,185	10,881	7,929	40,608	−3,012
89,867	4,319	8,174	6,926	45,946	−2,767
86,819	5,486	5,817	5,833	51,328	−2,490
83,514	6,637	3,830	4,697	56,682	−2,180
79,969	7,667	2,235	3,556	61,936	−1,828
76,127	8,535	1,048	2,452	67,016	−1,393
71,984	9,283	0,292	1,436	71,940	−0,806
67,594	9,926	0,000	0,586	76,798	−0,133
63,003	10,462	0,333	−0,110	81,551	0,448
58,264	10,890	1,322	−0,774	86,049	0,835
53,427	11,204	2,834	−1,439	90,145	0,986
48,543	11,402	4,827	−2,071	93,671	0,892
43,665	11,483	7,262	−2,639	96,468	0,625
38,844	11,446	10,104	−3,112	98,449	0,317
34,133	11,291	13,333	−3,431	99,616	0,086

$c_{Mo} = -0.1853$, $\beta_o = 7.05°$ (direction of zero lift relative to the x axis).

TABLE 2. PROFILE STF 863-615 (Fig. 2).

100 x	100 y	100 x	100 y	100 x	100 y
100,000	0,000	30,708	10,253	18,956	−2,493
99,640	0,119	26,312	9,744	23,174	−2,847
98,616	0,504	22,132	9,140	27,652	−3,142
97,051	1,167	18,210	8,449	32,337	−3,368
95,056	2,051	14,586	7,687	37,174	−3,515
92,689	3,067	11,297	6,866	42,104	−3,569
89,958	4,145	8,373	6,003	47,067	−3,512
86,869	5,272	5,846	5,117	52,003	−3,321
83,491	6,453	3,738	4,229	56,841	−2,915
79,933	7,622	2,075	3,363	61,682	−2,171
76,226	8,632	0,873	2,551	66,716	−1,223
72,280	9,417	0,158	1,838	71,891	−0,344
68,065	10,034	0,032	1,304	77,007	0,338
63,636	10,514	0,570	0,850	81,897	0,794
59,041	10,859	1,729	0,352	86,418	1,020
54,327	11,073	3,437	−0,161	90,446	1,034
49,545	11,157	5,658	−0,672	93,861	0,868
44,743	11,112	8,359	−1,170	96,559	0,591
39,971	10,944	11,503	−1,646	98,481	0,299
35,276	10,655	15,050	−2,090	99,623	0,081

$c_{M_0} = -0{,}1792$, $\beta_0 = 7{,}03°$

TABLE 3. PROFILE STE 871-514 (Fig. 18).

/260

100 x	100 y	100 x	100 y	100 x	100 y
100,000	0,000	28,155	8,762	20,200	— 3,506
99,626	0,095	23,780	8,321	24,599	— 3,791
98,562	0,412	19,660	7,797	29,259	— 4,027
96,925	0,970	15,839	7,197	34,125	— 4,206
94,815	1,717	12,359	6,532	39,140	— 4,325
92,276	2,594	9,255	5,812	44,244	— 4,379
89,340	3,578	6,565	5,049	49,378	— 4,360
86,086	4,666	4,320	4,257	54,482	— 4,261
82,635	5,780	2,560	3,436	59,493	— 4,069
79,014	6,755	1,295	2,561	64,353	— 3,771
75,123	7,523	0,471	1,634	68,994	— 3,302
70,930	8,144	0,049	0,744	73,489	— 2,564
66,490	8,650	0,059	0,039	77,995	— 1,678
61,852	9,043	0,678	— 0,496	82,452	— 0,883
57,067	9,327	1,972	— 0,996	86,676	— 0,288
52,185	9,499	3,827	— 1,484	90,508	0,089
47,260	9,562	6,207	— 1,951	93,817	0,260
42,343	9,516	9,074	— 2,392	96,490	0,263
37,486	9,365	12,390	— 2,801	98,437	0,165
32,740	9,112	16,114	— 3,174	99,610	0,050

$c_{M_0} = -0{,}1199$, $\beta_0 = 4{,}66^\circ$

REFERENCES

1. Abbott, I.H., A.E. Von Doenhoff, and C.S. Stivers, Jr., "Summary of airfoil data," NACA Rep. 824 (1945).

2. Lighthill, M.J., "A new method of two-dimensional aerodynamic design," ARC R. & M., 2112 (1945).

3. Truckenbrodt, E., "Calculation of a profile with specified velocity distribution," Ing.-Arch. 19, 365-377 (1951).

4. Eppler, R., "Direct calculation of airfoils from pressure distribution," Ing.-Arch. 25, 32-59 (1957).

5. Wortmann, F.X., "A contribution to the design of laminar profiles for sailplanes and helicopters," Z. Flugwiss. 3, 333-345 (1955).

6. Walz, A., "Application of the law of conservation of energy by Wieghardt on one-parameter velocity distribution in a duct in laminar boundary layers," Ing.-Arch. 16, 243-248 (1948).

7. Walz, A., Nouvelle méthode approchée de calcul des couches limites laminaire et turbulente en écoulement compressible [New approximation method of calculation of laminar and turbulent boundary layers in compressible flow], Publications scientifiques et techniques du ministère de l'air, No. 309, Paris, 1956.

8. Wieghardt, K., "On the calculation of two-dimensional and axially symmetric boundary layers with continuous suction," Ing.-Arch. 22, 368-377 (1954).

9. Truckenbrodt, E., "A quadrature method for calculating the laminar and turbulent friction layer for two-dimensional and axially symmetric flow," Ing.-Arch. 20, 211-228 (1952).

10. Schlichting, H. and W. Pechau, "Increase of lift of airfoils by means of continuously distributed suction," Z. Flugwiss. 7, 113-119 (1959).

11. Eppler, R., "Calculation of boundary layer by means of digital computers," Lecture at the Third European Aeronautics Convention, Brussels, September 1958; Report MN 4 of the Bölkow Entwicklungen KG, Ottobrunn near Munich.

12. Eppler, R., "Boundary layer separation and dead water formation," Jahrbuch 1957 der WGL [1957 Yearbook of the WGL], pp. 238-247.

13. Kraemer, K., "Wind tunnel measurements on the profile EC 86(-3)-914," Report 56/A/05 of the Aerodynamic Test Facility, Göttingen (1956).

14. Raspet, A. and D. Gyorgyfalvy, "The 'Phönix' -- A solution for optimal cross-country sailplane flight," Z. Flugwiss. 8, 260-266 (1960).

15. Kraemer, K., "Wind tunnel measurements on ten profiles," Report 57/A/39 of the Aerodynamic Test Facility, Göttingen (1957).

16. Kraemer, K., "Wind tunnel measurements on two profiles with sucking away of the wall boundary layer in the vicinity of the wing root," Report 58/A/36 of the Aerodynamic Test Facility, Göttingen (1958).